

EFFECT OF ANION, pH, AND TEMPERATURE ON THE DISSOLUTION BEHAVIOR OF ALUMINUM OXIDE FILMS

Hochun Lee and Hugh S. Isaacs

Department of Materials Science
Brookhaven National Laboratory, Upton, NY 11973

ABSTRACT

The growth and dissolution behavior of oxide film on abraded pure Al has been investigated using cyclic polarization and has been found to be highly dependent on solution chemistry and temperature. The nature of the anions, borate, chromate, phosphate, and sulfate, at pH 3 to 11, and temperatures 0 to 60 °C were examined. In near neutral solutions the dissolution behavior was greatly affected by each anion. In borate and chromate solutions at near neutral pH and room temperature, the currents continued to decrease with each subsequent cycle due to oxide thickening. In contrast, a significant rate of oxide dissolution occurred to produce reproducible repetitive curves during subsequent cycles in a phosphate and sulfate. Sulfate also produced a distinctly different mode during high field oxide growth. In increasing acidic (pH < 4) or basic (pH >9) solutions the oxide dissolution rate increased rapidly. The oxide dissolution rate was always enhanced with increasing temperature. At high pH (>9) or elevated temperature (60 °C), a current maximum was observed in chromate, due to a diffusion controlled monochromate ion enhanced dissolution reaction at the oxide/solution interface.

INTRODUCTION

Extensive studies have been performed on the adsorption and incorporation of anions at surface oxide films with the view of corrosion protection.¹⁻³ Anion adsorption and/or incorporation affects the dissolution rate, the degree of hydration, and surface charge.⁴⁻⁶ Adsorption/incorporation of aggressive anions such as halide has been suggested to cause dissolution and thinning of the oxide film, and could play an important role in initiation of localized breakdown of passivity.⁷⁻⁹ Systematic studies of the dissolution behavior of Al oxide films, however, are infrequent despite its importance in understanding the general corrosion and initiation of localized corrosion.

The dissolution behavior of Al oxide films has been investigated mainly in acidic solutions where porous oxide film is formed^{3,10,11} and in alkaline solutions in the development of Al-air battery.^{12,13} The solubility of Al oxides is markedly increased under both acidic and alkaline conditions.^{14,15} However, little information is available on the dissolution process in the neutral pH range (pH 5-9). Deltombe and Pourbaix¹⁴ presented a diagram of the solubility variation of several crystalline Al oxides vs. solution pH as controlled by expected solubility product characteristics. However, this fails to reflect the pH dependence in the

near neutral pH region. Alwitt¹⁶ reported a experimental results with a solubility in the near neutral region around 10^{-5} M, because of the difficulty in obtaining reliable measurements at the low rate of dissolution in mild conditions with non-aggressive anions in near neutral solutions at room temperature.

The stable dissolved species are known to be $\text{Al}(\text{H}_2\text{O})_6^{3+}$ and $\text{Al}(\text{OH})_4^-$ in acidic and basic solutions, respectively.¹⁵ However, the dissolved product in the intermediate pH region has been known to vary from AlOH^{2+} to several polynuclear species depending on the experimental conditions such as pH, temperature, anionic species, and ionic strength.¹⁵ In addition, the nature of anion affects dissolution behavior probably by the formation of Al-anion hydroxide complex.^{5,15-19}

Recently, we demonstrated the applicability of simple cyclic polarization measurements to determine the growth and dissolution characteristics of pure Al oxide in near neutral borate, chromate, phosphate, and sulfate solutions.¹⁹ The results offered insights into the interaction of anions with the oxide film. The aim of this study is to extend our previous report to examine the effect of pH, temperature, and the nature of anions on the characteristics of oxide growth and dissolution by using the cyclic polarization technique.

EXPERIMENTALS

A high purity Al (99.9999 %, Cominco Electronic Materials) square rod was used with a cross sectional area of 1 cm^2 . The surface of Al rod was first anodized to 100 V at a constant current density of 2 mA/cm^2 in borate buffer (pH 8.0) for electrical insulation. Prior to testing, the cross section of the rod was abraded down to a 600 grit SiC paper while wetted with deionized (DI) water. After the abrasion, it was washed well with DI water and dried in air. The abraded end of Al rod was immersed in solution to about 2 mm depth during the measurements. The solutions were made with analytical grade reagents and $18 \text{ M}\Omega$ DI water. Concentration of all the solutions was fixed as 0.5 M in anion concentration but having various compositions to obtain desired pH values : phosphate solution (NaH_2PO_4 / Na_2HPO_4), borate solution (H_3BO_3 / $\text{Na}_2\text{B}_4\text{O}_7$), chromate solution (K_2CrO_4 / $\text{K}_2\text{Cr}_2\text{O}_7$), and sulfate solution (Na_2SO_4). In some cases, pH was adjusted by addition with conjugated acid or hydroxide.

During testing the solutions temperature was held within $\pm 0.2 \text{ }^\circ\text{C}$ and were freely exposed to air. The scan rate was fixed to 5 mV/s . A saturated mercury sulfate reference electrode (0.39 V more positive than a saturated calomel electrode) and platinum counter electrode were used.

RESULTS

Anion Dependence

Figure 1 shows the cyclic polarization curves of abraded pure Al in borate, phosphate, sulfate, and chromate solutions of pH 7.0 at $20 \text{ }^\circ\text{C}$. In the

borate (Fig. 1a), the current increases rapidly and then reaches a plateau region during the first anodic scan. When the scanning direction is reversed at -0.3 V the current drops rapidly and approaches zero. During the second anodic scan, the current remains low until -0.8 V and then increases slightly. Note that the current at the positive potential limit (-0.3 V) for the second and the subsequent cycles continues to decrease. This is because the oxide film thickness increases during each cycle. The polarization behavior in the borate can be accounted for in terms of the high field conduction model^{3,10,20} without dissolution of oxide. More detail can be found in our previous report.¹⁹

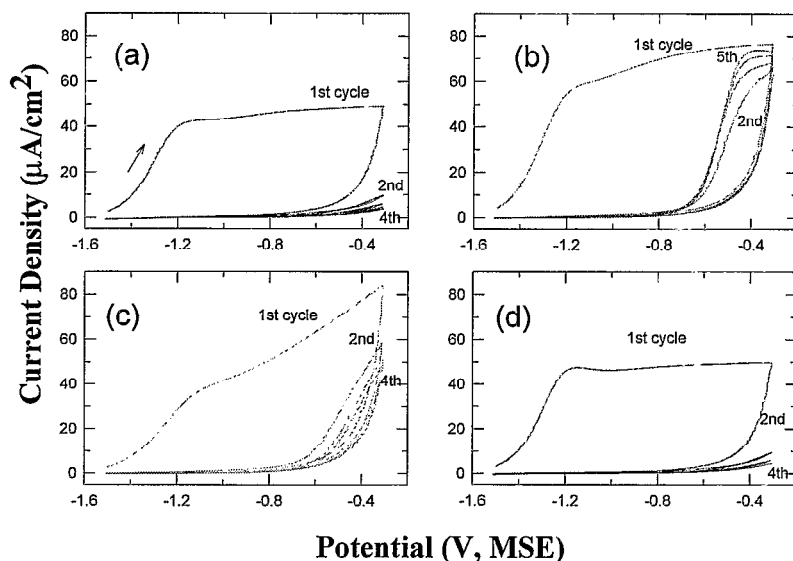


Figure. 1 Cyclic polarization characteristics of freshly abraded Al in 0.5 M (a) borate, (b) phosphate, (c) sulfate, and (d) chromate (pH 7.0)

In phosphate (Fig. 1b), the current response in the first cycle is similar to that in the borate (Fig. 1a) except that the current density at the plateau is somewhat increased. However, the current again increases to a comparable value during the subsequent cycles. At the higher potentials the current shows virtually the same dependence after the fifth cycle. The repeated high currents indicate additional anodic oxide formation taking place to compensate the loss of oxide caused by dissolution. The shape of the curves can be accounted for in terms of the high field conduction model with oxide dissolution.¹⁹

However, in the sulfate (Fig. 1c), the first cycle shows no plateau and the current continues to rise almost linearly with potential reaching above $80 \mu\text{A}/\text{cm}^2$ before the scan direction is reversed. The current in subsequent cycles continues to decrease until the fourth cycle and only then becomes repetitive. The latter behavior implies that oxide dissolution is again occurring and reaches a dynamic steady state. The direct application does not account for the unique behavior in the sulfate and further investigation is in progress to reveal the reason of the distinctively different behavior in the sulfate. This behavior is also seen in nitrate solutions.

The current in the chromate (Fig. 1d) is almost the same as that in the borate (Fig. 1a) which indicates oxide growth with no discernable dissolution at pH 7 and 20°C.

pH Dependence

Figure 2 shows the polarization curves in acidic and basic solutions. The pH has dramatic effects on the anodic oxide growth in borate solutions. In pH 4.1 borate (solid line in Fig. 2a), the currents observed are much lower than those at higher pH. The currents are smaller when the potential is decreased after reaching the highest potential and continue to decrease for each subsequent cycle. This behavior indicates oxide growth kinetics dominate the growth process and produce a very different oxide film that that grown at pH 7. The poor dissociation of the boric acid also results in a high solution resistance which, because of resistance polarization could reduce the oxide formation current well below that in the borate of pH 7.0 (Fig. 1a). However, If were the only cause and the nature of the oxide did not change, the forward and reverse currents would be the same until sufficient charge had passed to thicken the oxide. The charge passed is considerably less than that at pH 7. Hence it is expected that the nature of the film must be different. The changes may be due to an increase in the ionic resistivity of the film or incorporation of borate giving a thicker film.

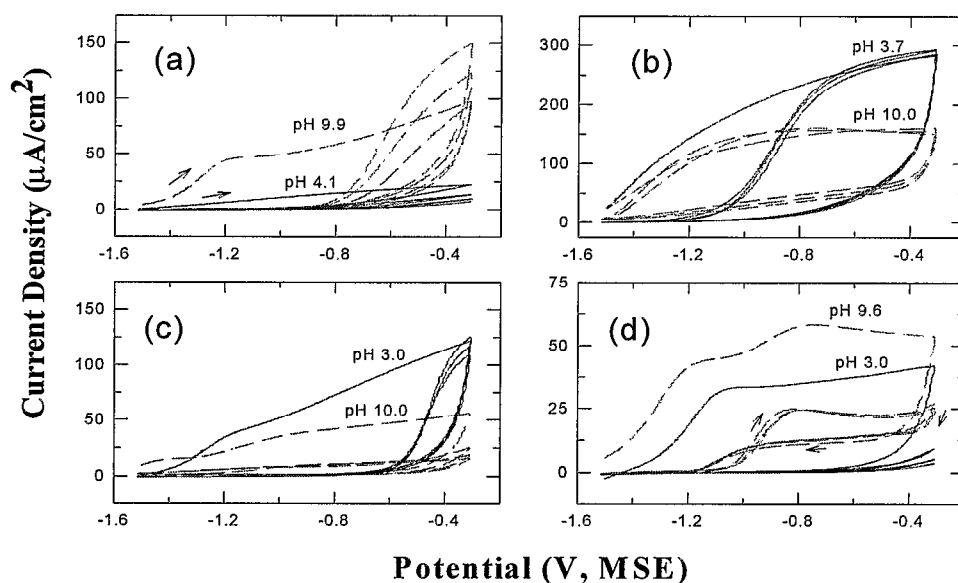


Figure. 2 Cyclic polarization characteristics of freshly abraded Al in 0.5 M (a) borate, (b) phosphate, (c) sulfate, and (d) chromate at acidic (---) and basic (----) solution.

In pH 9.9 borate, the plateau region disappears and the current continues to increase. When the scanning direction is reversed during the first anodic scan (dashed line in Fig.2a), a behavior characteristic of the neutral pH 7 sulfate (Fig. 1c) is seen. In addition, the high current and the hysteresis during subsequent anodic scan shows that oxide dissolution is taking place at significant rates.

Figure 2b shows the polarization curves in the phosphate solutions of pH 3.7, 7.0 and 10.0. In both acidic and alkaline conditions, the current at the first cycle is increased significantly compared to that in the neutral solution (Fig. 1b). The subsequent cycles also show large current and pronounced hysteresis, indicating high dissolution rate in the acidic and the alkaline phosphates.

Figure 2c shows the results in the sulfate solutions of pH 3.0, 7.0 and 10.0. The current response at pH 3.0 (solid line) is somewhat similar to that at pH 7.0 (Fig. 1c) with a considerably increased current density. This implies increased dissolution rate in an acidic sulfate solution. However, the slope in the first cycle at pH 10.0 (dashed line) is smaller than those in the neutral or acidic solutions. Moreover, the current during the subsequent cycles starts increasing from -1.5 V but remains quite low to -0.3 V. Increased amount of OH^- ion seems to suppress the sulfate characteristics probably by the competition with sulfate ion.

Figure 2d shows results in the chromate solutions of pH 3.9, 7.0 and 9.2. In the chromate of pH 3.0 (solid line), the first cycle is similar to that in pH 7.0 except that the current density is somewhat decreased and the current starts from negative value. However, the polarization behavior in pH 9.2 (dashed line) shows very different from those in acidic and neutral solutions. During the first anodic scan, current bump is observed around -0.85 V and the current remains quite high until about -1.2 V at the reversing cathodic scan. This additional dissolution current is again clearly seen during the subsequent cycles at the same potential.

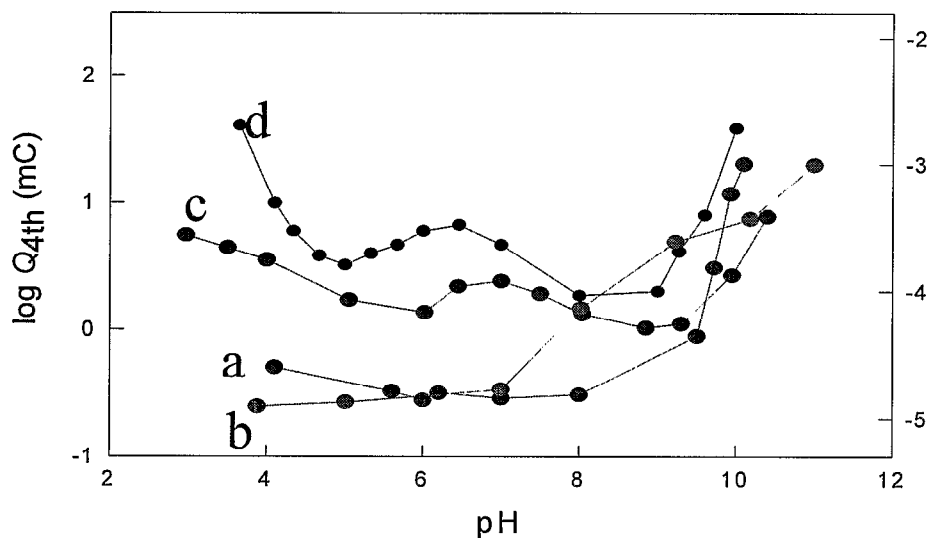


Figure. 3 pH dependence of dissolution rate and solubility in (a) borate, (b) phosphate, (c) sulfate, and (d) chromate.

Figure 3 summarizes the pH dependence of dissolution rate. The charge change during the fourth cycle, Q_{4th} is used as a measure of dissolution rate. The concentration of soluble Al species is also shown, which was calculated from

$$[\text{soluble Al species}] = Q_{4\text{th}} / nFV \quad [1]$$

$$V = A(2Dt)^{1/2} \quad [2]$$

where n is the number of electrons transferred to dissolve the oxide, F the Faraday constant, V the effective volume for soluble Al species, A the surface area, D diffusion coefficient (assumed to be $10^{-5} \text{ cm}^2/\text{s}$), and t the time for 1 cycle. With the exception of acidic borate and acidic chromate, $Q_{4\text{th}}$ increases as pH decreases below pH 5 and pH increases above pH 9, which is an expected behavior based on the results of Poubaix¹⁵ and Alwitt¹⁶. However, the dissolution rate in the intermediate pH range shows very unusual behavior. Note that the phosphate and sulfate show a local maximum around pH 6.5 and 7.0, respectively. For example, pH change from 6 to 8 in the phosphate results in five times smaller dissolution rate. When this result is compared with the plot of Poubaix¹⁵ and Alwitt¹⁶, fairly good agreement is noticed in both acidic and basic regions. But the dissolution rate in the near neutral phosphate and sulfate are somewhat larger, which seems to be due to the dissolving power of those anions.

Temperature dependence

Figure 4 shows the polarization curves at low and high solution temperature. In the borate (Fig. 4a), the curve at 0 °C (solid line) looks almost the same as that at 20 °C except somewhat decreased current density. However, the curve at 50 °C shows no plateau during the first scan and the subsequent cycles show considerable width, which are characteristics of the sulfate and the

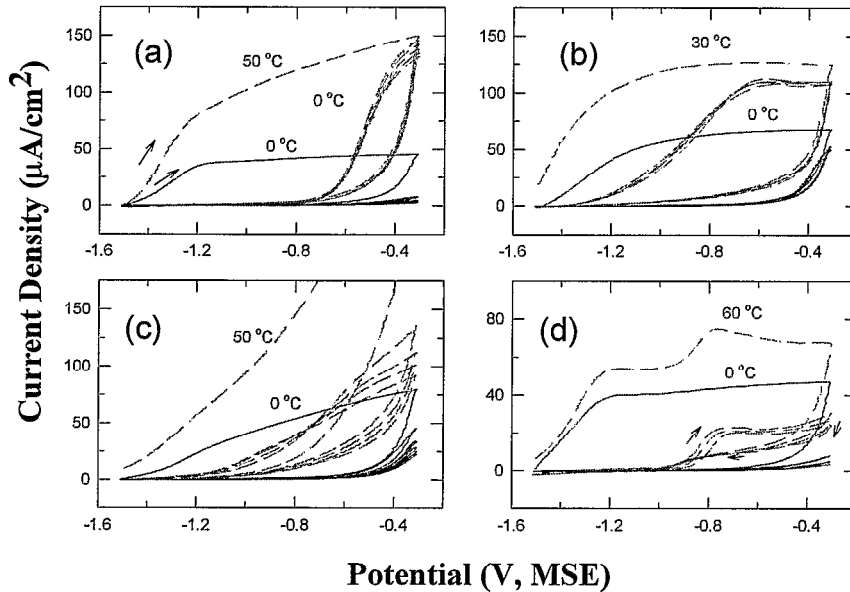


Figure. 4 Cyclic polarization characteristics of freshly abraded Al in 0.5 M (a) borate, (b) phosphate, (c) sulfate, and (d) chromate at low (---) and high (----) temperatures.

phosphate, respectively. In the phosphate (Fig. 4b), the current in the plateau of the first cycle and the width of subsequent cycles increase as temperature

increases. In the sulfate (Fig. 4c), steeper slope at the first cycle and wider width at the subsequent cycles are observed at 50 °C compared at 0 °C. In the chromate (Fig. 4d), the polarization behavior at 0 °C looks nearly the same as that at 20 °C. However, additional current bump begin to appear around -0.85 V at the anodic scans above 60 °C. Note that this behavior is very similar to that in the chromate of high pH (Fig.2d).

Figure 5 shows the temperature dependence of the dissolution rate. Again Q_{4th} is regarded as a measure of dissolution rate and the concentration of soluble Al species was calculated according to Eq. 1 and 2. Generally, the dissolution rate is increasing with the solution temperature. For example, 40 °C of temp change gives about ten times solubility increase.

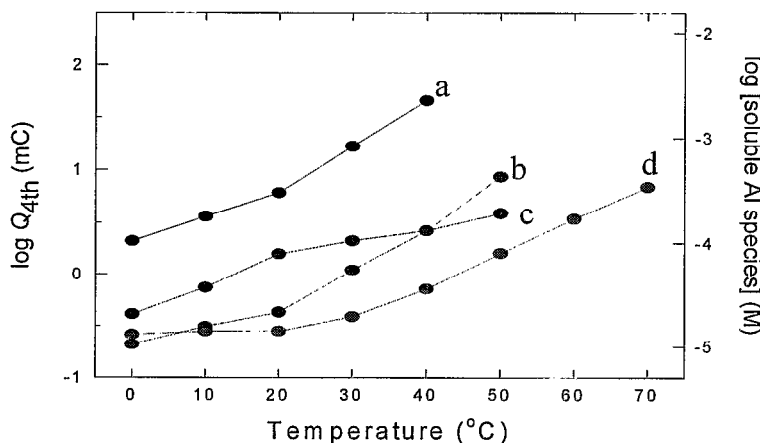


Figure. 5 temperature dependence of dissolution rate and solubility in 0.5 M (a) borate, (b) phosphate, (c) sulfate, and (d) chromate

Effects of convections

In order to determine the effect of mass transfer a rotating disk electrode (RDE) has been employed. Figure 6 shows the polarization curves at 1600 rpm. The polarization curves in the borate and the chromate (Fig. 6a and d, respectively) are not affected much by enhanced convection. However, in phosphate (Fig. 6b), the first cycle shows no plateau region and the subsequent cycles show wider current width, which implies that oxide dissolution is increased with enhanced mass transfer. In contrast, the slope in the first cycle and the current in the subsequent cycles are decreased in the sulfate, which indicates the oxide

The relation between the dissolution rate (as determined from Q_{4th}) and the square root of rotation speed ($\omega^{1/2}$). In the phosphate, the dissolution rate first increases rapidly and then reaches a steady value. In the sulfate the dissolution rate decreases slightly with increasing $\omega^{1/2}$. In the borate and the sulfate, the dissolution rate does not change much over the range of 0 ~ 1600 rpm. The effect dissolution is disturbed.

of enhance mass transfer is most prominent in the alkaline chromate of pH 9.6. The current bump at 400 rpm is about four times larger than that at 0 rpm (Fig.

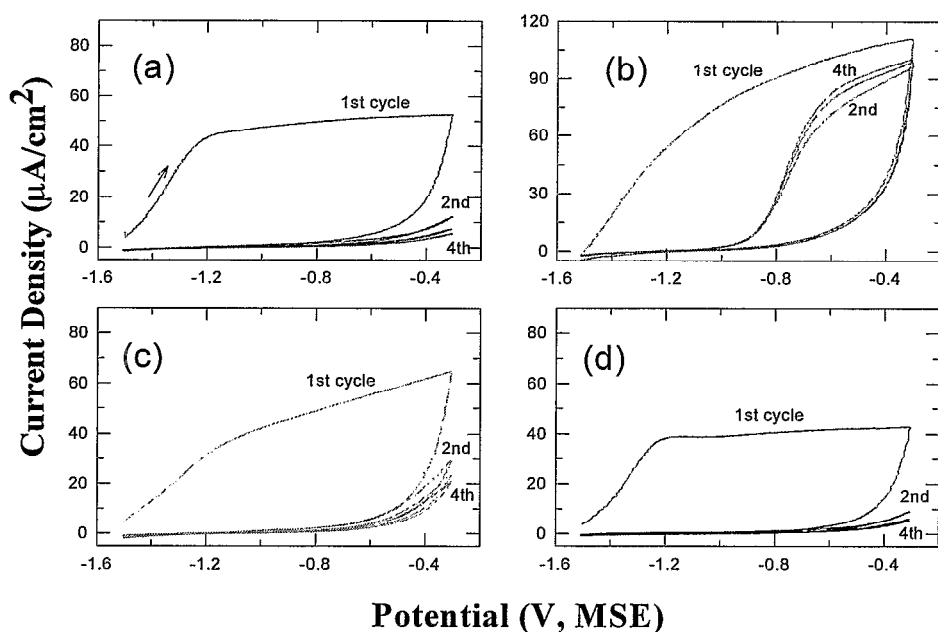


Figure. 6 Cyclic polarization characteristics of freshly abraded Al in 0.5 M (a) borate, (b) phosphate, (c) sulfate, and (d) chromate, rpm=1600

7a). Fig. 7b shows that both Q_{4th} and the current bump at the 2nd anodic scan are in the linear relationship with $\omega^{1/2}$ up to $50 \text{ rpm}^{1/2}$, which indicates fast kinetics for the reaction between the chromate and the oxide to produce the soluble

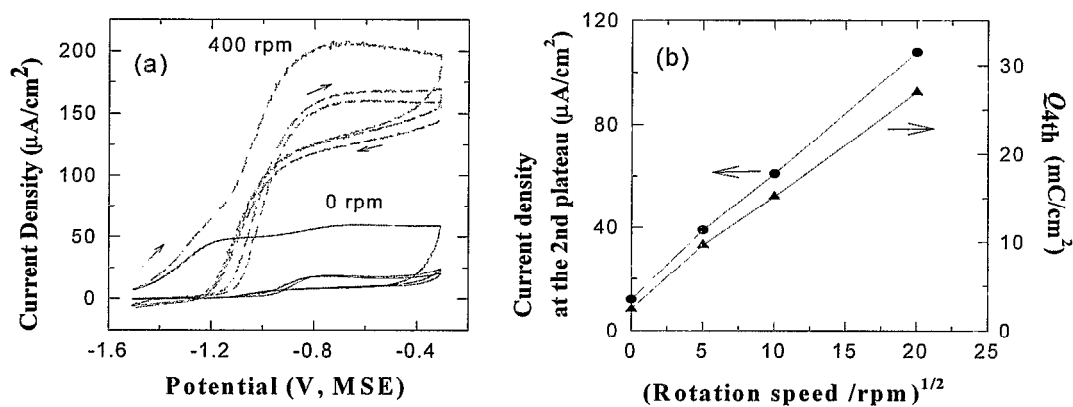


Figure 7 (a) Cyclic polarization characteristics of freshly abraded Al in 0.5 M chromate (pH =9.6) at 0 and 400 rpm. (b) current density at the plateau of the 2nd anodic scan and Q_{4th} vs. $\omega^{1/2}$.

products associated with the current maximum.

DISCUSSION

A simple but useful model has been proposed to express the influence of various surface species such as proton, hydroxide, and organic inorganic ligands on dissolution rate of oxides.^{18,21} Similarly, dissolution rate (R_{net}) can be assumed to consist of proton (R_{H^+}) or hydroxide-promoted (R_{OH^-}) and anion-promoted (R_{X}) ones, which are independent and parallel to each other.

$$R_{\text{net}} = R_{\text{H}^+} + R_{\text{OH}^-} + R_{\text{X}} \quad [3]$$

$$R_{\text{H}^+} = k_{\text{H}^+} [\text{H}^+] \quad [4]$$

$$R_{\text{OH}^-} = k_{\text{OH}^-} [\text{OH}^-] \quad [5]$$

$$R_{\text{X}} = k_{\text{X}} [\text{Al-X}] \quad [6]$$

where $[\text{Al-X}]$ is the surface concentration of the aluminum anion complex.

Regarding on the dissolution rate dependence on pH and temperature, following hypothesis can be made.

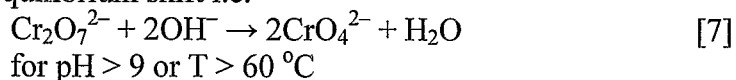
- (1) At acidic (pH < 5) and alkaline (pH > 9) conditions, R_{net} is governed by R_{H^+} and R_{OH^-} , respectively. This accounts for monotonous increase of dissolution rate in acidic and alkaline pH regions.
- (2) R_{X} becomes dominant at intermediate pH region (pH 5 ~ 9), where the pH dependence of dissolution rate is rather complex. Both k_{X} and $[\text{Al-X}]$ are affected by the nature of anion and pH.
- (3) k_{H^+} , k_{OH^-} , and k_{X} increase with increasing temperature, which explains the relationship between dissolution rate and temperature.

No reported experimental results have been found on the temperature dependence of the solubility of passive oxide films on Al. However, according to Pourbaix diagrams at elevated temperatures, the most noticeable change is that the equilibrium between Al oxide and aluminate ion (AlO_2^-) shifts to lower pH and expands the region of aluminate.²² Hence thermodynamics predicts that Al oxide dissolution is favored at higher temperatures. In addition, the dissociation of water increases substantially at elevated temperatures and increases in proton and hydroxide ion will cause additional increase in dissolution rate.¹⁵

Changes in convection enables a separation to be made between surface controlled or mass transport controlled dissolution rates of the oxide. can be n varying the convection rate, the dissolution product from the surface of Al is removed and dissolution rate increases in the phosphate until kinetic limitation is reached. However, no significant effect is observed in the borate and the chromate, which reflects very slow kinetics for oxide dissolution in these media. In the sulfate, enhanced convection removes the dissolution product from the surface of Al and decreases dissolution rate, which implies auto-catalytic nature of the dissolution process in the sulfate.

Under high pH (>9) or high temperature (60 °C), a current maximum was observed in the chromate. It is known that increasing pH shifts the equilibrium toward mono-chromate,⁴ (CrO_4^{2-}). The current maximum is apparently due to a diffusion-controlled oxide dissolution reaction with the monochromate, CrO_4^{2-} , at

the oxide/solution interface and not the dichromate, $\text{Cr}_2\text{O}_7^{2-}$. Based on the similarity between the polarization behavior at high pH (Fig. 2d) and high temperature (Fig. 4d), it is apparent that increasing temperature also due to the same equilibrium shift i.e.



CONCLUSIONS

1. Simple cyclic polarization measurement offers a rapid and sensitive method for characterizing Al oxide dissolution over a wide range of solution composition, pH, and temperature. The slow oxide dissolution rate in the intermediate pH range (pH 5-9) can be assessed in addition to the high rates in acidic and alkaline media.
2. In close to neutral solutions and at room temperature, borate and chromate solutions show a low oxide dissolution rate, whereas phosphate and sulfate solutions show a relatively high rate.
3. The oxide growth in sulfate does not follow a simple high field conduction behavior unlike the behavior in the borate, chromate and phosphate solutions.
3. Increasing temperature enhances the dissolution rate in all the cases.
4. With enhanced convection at pH 7 and room temperature, phosphate solution shows increasing oxide dissolution due to a mass transport limited process in solution. Borate and chromate do not show any solubility while sulfate shows slightly decreasing dissolution rate with increased flow rates
5. A current maximum is observed in the alkaline ($\text{pH} > 9$) and elevated temperatures ($> 60^\circ\text{C}$) in chromate, due to the surface reaction of mono-chromate ions at the oxide/ solution interface.

ACKNOWLEDGMENT

This work was conducted at Brookhaven National Laboratory under the auspices of Department of Energy, Division of Materials Sciences, Office of Science under contract No. DE-AC02-98CH10886.

REFERENCES

1. Z. Németh, L. Gáncs, G. Gémes, and A. Kolics, *Corros. Sci.*, **40**, 2023 (1998).
2. G. E. Thompson and G. C. Wood, in *Corrosion: Aqueous Processes and Passive Films*. J. C. Scully, Editor, p. 271, Academic Press, London (1983).
3. P. Skeldon, K. Shimizu, and G. C. Wood, *J. Electrochem. Soc.*, **143**, 74 (1996).
4. M. Kendig, R. Addison, and S. Jeanjaquet, *J. Electrochem. Soc.*, **146**, 4419 (1996).
5. H. Konno, S. Kobayashi, H. Takahashi, and M. Nagayama, *Corros. Sci.*, **22**, 913 (1982).
6. E. McCafferty, *Corros. Sci.*, **37**, 481 (1995).
7. H. H. Strehblow, in *Corrosion Mechanism in Theory and Practice*, P. Marcus and J. Oudar, Editors, p. 201, Marcel Decker, Inc., New York (1995).
8. K. E. Heusler and L. Fischer, *Werst. Korros.*, **27**, 551 (1976).
9. S. Y. Yu, W. E. O'Grady, D. E. Rammaker, and P. M. Natishan, *J. Electrochem. Soc.*, **147**, 2952 (2000).
10. J. W. Diggle, T. C. Downie, and C. W. Goulding, *Chem. Rev.*, **69**, 365 (1969).
11. J. W. Diggle, in *Oxides and Oxide Films*, Vol. 2, J. W. Diggle, Editor, p. 281, Marcel Decker, Inc., New York (1973).
12. O. R. Brown and J. S. Whitley, *Electrochim. Acta.*, **32**, 545 (1987).
13. D. Chu and R. F. Savinell, *Electrochim. Acta.*, **36**, 1631 (1991).
14. E. Deltombe and M. Pourbaix, *Corrosion*, **14**, 496t (1956).
15. R. S. Alwitt, in *Oxides and Oxide Films*, Vol. 4, J. W. Diggle and A. K. Vijh Editors, p. 169, Marcel Decker, Inc., New York (1976).
16. P. L. Hayden and A. J. Rubin, in *Aqueous-Environmental Chemistry of Metals*, A. J. Rubin, Editor, p. 317, Ann Arbor Science, Ann Arbor, (1974).
17. J. J. Randall and W. J. Bernard, *Electrochim. Acta.*, **20**, 653 (1975).
18. S. T. Kraemer, V. Q. Chiu, and J. G. Hering, *Environ. Sci. Technol.*, **32**, 2876 (1998).
19. H. Lee, F. Xu, C. S. Jeffcoate, and H. S. Isaacs, *Electrochem Solid-State Lett.*, **4**, B31 (2001).
20. M. M. Lohrengel, *Mat. Sci. and Eng.*, **R11**, 243 (1993).
21. G. Furrer and W. Stumm, *Geochim. Cosmochim. Acta*, **52**, 1139 (1986).
22. D. Macdonald and P. Butler, *Corros. Sci.*, **13**, 259 (1973).